Magnetic-field and spin-orbit interaction in restricted geometries: Solvable models

Yigal Meir
Department of Physics, Massachusetts Institute of Technology, Cambridge, Massachusetts 02139

O. Entin-Wohlman
Raymond and Beverly Sackler Faculty of Exact Sciences, School of Physics and Astronomy, Tel Aviv University, Ramat Aviv, Tel Aviv 69978, Israel

Yuval Gefen
Department of Physics, Weizmann Institute of Science, Rehovot 76100, Israel
(Received 5 February 1990; revised manuscript received 5 June 1990)

Properties of a two-dimensional degenerate gas of noninteracting electrons, subject to a perpendicular magnetic field, are investigated by studying two solvable models. These models amount to restricted geometries in the plane. The first reveals three types of oscillations (as a function of the applied field) of thermodynamic quantities: de Haas–van Alphen (dHvA) oscillations, Aharonov-Bohm (AB) oscillations, and oscillations related to correlations among energy levels associated with different Landau levels. In the second model the latter correlations are absent, and the third kind of oscillations is manifested as nonperiodic fluctuations of the thermodynamic quantities at hand. Accounting for spin-orbit (s.o.) interaction, it is found that the dHvA oscillations split into a sum of "spin-up" and "spin-down" branches. The expressions for the AB oscillations acquire "universal" s.o. reduction factors. Introducing a modification of the second model (which is treated using a WKB approach), an enhanced s.o. coupling, and consequently a larger s.o. effect, is obtained. Both the phenomena of quantum Hall effect and longitudinal conductance quantization are demonstrated in the two models, with AB oscillations superimposed on the conductance plateaus.

I. INTRODUCTION

The behavior of a two-dimensional degenerate electron gas in a perpendicular magnetic field has revealed many interesting physical phenomena. In such a field the free-electron eigenenergies cluster into Landau levels, and this periodic quantization leads to features such as the de Haas–van Alphen (dHvA) effect[1] and the quantized Hall effect (QHE).[2] The finite size of the system at hand is crucial to the understanding of these phenomena.[3] Indeed, much effort was directed towards solutions of finite-size systems subject to a magnetic field H. One may write a formal solution in terms of hypergeometric functions; in this case the energy levels are obtained numerically[4] and it is rather difficult to gain physical insight as to the way the spectrum is manifested in, e.g., thermodynamic properties. Furthermore, certain ingredients, e.g., electron-electron correlations, are often neglected. These also include spin-orbit (s.o.) interaction, proportional to the gradient of the potential acting on the electron, which is usually ignored, though the gradient may be rather large near the boundaries.

The magnetization of a finite-size system exhibits dHvA oscillations as a function of $1/H$, which result from the interplay between the increase in the energy of each Landau level and the increase in the degeneracy of these levels as the magnetic field is increased. These oscillations correspond to periodic intersections of the Fermi energy μ by a Landau level. (A similar description can be given for a system with a constant number of electrons.) It has been suggested[5,6] that one should observe Aharonov-Bohm[7] (AB) oscillations, with a period $\phi_0 \equiv hc/e$, as a function of the total flux through the system, superimposed on the dHvA oscillations. This result is based upon a Wentzel-Kramers-Brillouin (WKB) approximation for a disc geometry, and numerical results for certain disordered systems.[6] When the magnetic flux through the system is increased by ϕ_0, the degeneracy of each Landau level is increased by unity as one edge state merges into the bulk (or, alternatively, another edge state crosses the Fermi energy.)

In this article we present two exactly solvable models which yield simple spectra, easily amenable to the calculation of various physical quantities. To simulate the boundaries, we introduce confining potentials and choose parameters representative of mesoscopic samples. We concentrate upon the effect of the boundaries on the orbital motion of the electron (and how this is manifested in the energy spectrum), disregarding Zeeman splitting. Operating at zero temperature, we derive an exact expression for the grand partition function. This facilitates calculations of various thermodynamic properties, in particular, the magnetization. We find that the magnetization shows AB oscillations superimposed on the dHvA ones. The explicit form of the magnetization allows us to discuss correlations among different Landau levels and how they affect the amplitude of the AB oscillations. We derive the quantization of the longitudinal conductance[8,9] and that of the Hall conductance in our constricted geometry. We find AB oscillations superimposed on the

 ©1990 The American Physical Society

standard Hall plateaus.

Adding the s.o. term to our Hamiltonians, we are still able to derive the spectra and the partition functions exactly. Using those, we investigate the effects of s.o. interaction upon the magnetization. This interaction leads to additional features in the dHvA and AB effects. The s.o. parameter in our model systems has to be chosen rather small. This is a consequence of the fact that, in these models, the confining potentials are parametrized by a single quantity, which determines both the "width" of the sample and the potential gradient near the boundary. We therefore introduce in Sec. V a more "realistic" confined geometry and analyze it using a WKB approximation. Within that approach, the value of the s.o. parameter turns out to be larger.

II. CONFINING POTENTIAL: FIRST EXAMPLE

We consider an independent degenerate electron gas in a two-dimensional system, subject to a radially symmetric confining harmonic potential and a perpendicular magnetic field H. The Hamiltonian is

$$\mathcal{H}=\frac{1}{2m}\left[\mathbf{p}-\frac{e\,\mathbf{A}}{c}\right]^2+\frac{m}{2}\omega_0^2 r^2 , \tag{2.1}$$

$\mathbf{A}$ being the vector potential. To relate the parameters of our model to those of a realistic two-dimensional mesoscopic sample of radius R, we choose the chemical potential μ such that

$$\mu=\tfrac{1}{2}m\omega_0^2 R^2 . \tag{2.2}$$

Given R and μ, ω_0 is determined such that the potential energy of the electron is equal to the Fermi energy. For the strong magnetic fields discussed in this paper, $\mathcal{H}\sim 1-10$ T, $\omega_c\equiv eH/mc\sim 10^{11}-10^{12}$ 1/sec, and $\hbar\omega_c\sim 10^{-4}-10^{-3}$ eV. (Here we have used the free-electron mass. In semiconductors, e.g., $GaAs/Al_{1-x}Ga_xAs$, this should be replaced by ~ 0.1 m, leading to $\hbar\omega_c\sim 10^{-3}-10^{-2}$ eV.) Considering a small number of Landau levels, μ is of the order of 1 meV. For our system to be mesoscopic (smaller than the phase breaking length), $R\sim 10^{-4}$ cm is a reasonable choice, which, by Eq. (2.2), implies $\omega_0\sim 10^{10}$ 1/sec $\ll\omega_c$. Such a model Hamiltonian has been shown to produce results consistent with experiments on quantum dots.[3]

The spectrum of (2.1) is well known. It is practically that of a two-dimensional harmonic oscillator [cf. Eq. (2.3) below]. To see this, it is convenient to choose the gauge $\mathbf{A}=\frac{1}{2}\mathcal{H}\times\mathbf{r}$ and substitute $\Psi(r,\theta)=\phi(r)e^{il\theta}$ for the solutions of the Schrödinger equation. It follows that ϕ obeys the one-dimensional equation

$$\left[-\frac{\hbar^2}{2m}\left[\frac{\partial^2}{2r^2}+\frac{1}{r}\frac{\partial}{\partial r}\right]+\frac{l^2\hbar^2}{2mr^2}+\frac{m}{2}\left[\frac{\omega_1}{2}\right]^2 r^2-\tfrac{1}{2}l\hbar\omega_2\right]\phi=E\phi , \tag{2.3}$$

with $\omega_1^2=\omega_c^2+4\omega_0^2$ and $\omega_2=\omega_c$ (ω_2 is defined for later convenience). Equation (2.3) yields the discrete spectrum

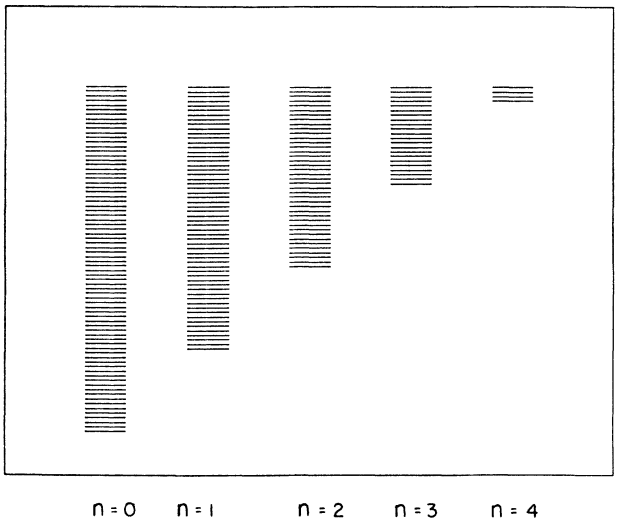

FIG. 1. Energy levels for model I; $\omega_c/\omega_0=4$. The levels within each n are indexed by the quantum number m, cf. Eq. (2.4b).

$$E_{nl}=(n+\tfrac{1}{2}+\tfrac{1}{2}|l|)\hbar\omega_1-\tfrac{1}{2}l\hbar\omega_2 , \quad n=0,1,2,\ldots,\ l=0,\pm1,\pm2,\ldots . \tag{2.4a}$$

This may be recast in the form

$$E_{nm}=(n+\tfrac{1}{2})\hbar\omega+(m+\tfrac{1}{2})\Delta,\quad n,m=0,1,2,\ldots , \tag{2.4b}$$

with $\omega=(\omega_1+\omega_2)/2$ and $\Delta=\hbar(\omega_1-\omega_2)/2$. The spectrum for $\omega_c/\omega_0=4$ is depicted in Fig. 1. Each Landau level [n in Eq. (2.4b)], degenerate in the absence of a confining potential, splits into a ladder of equally spaced (with spacing Δ) sublevels (m). The confining potential which varies smoothly in space removes the degeneracy of the bulk Landau levels. By contrast, sharp boundary conditions leave most of the bulk levels degenerate, lifting the degeneracy of few states at the edges. From this point of view all eigenstates in our case are edge states.

We now use the spectrum to calculate thermodynamic properties of our model at $T=0$; these are derived from the grand partition function

$$\ln Q=\sum_{n=0}^{\infty}\sum_{m=0}^{\infty}\ln(1+e^{\beta(\mu-E_{nm})}),\quad \beta\equiv 1/k_B T . \tag{2.5}$$

Employing the Poisson summation formula

$$\sum_{m=0}^{\infty} f(m)=\sum_{p=-\infty}^{\infty}\int_0^{\infty} f(x)e^{2\pi ipx}dx+\tfrac{1}{2}f(0) , \tag{2.6}$$

we find, in the $T\to 0$ ($\beta\to\infty$) limit,

$$\ln Q=\beta\Delta\sum_{n=0}^{n_0}\left[\frac{1}{2}X_n(X_n+1)-\sum_{p=1}^{\infty}\frac{1}{2\pi^2p^2}[\cos(2\pi pX_n)-1]\right] , \tag{2.7a}$$

where $X_n \equiv [\mu-(n+\frac{1}{2})\hbar\omega-\frac{1}{2}\Delta]/\Delta$ and n_0 is the index of the highest occupied Landau level, given by the largest integer that satisfies $X_n \geq 0$. Equation (2.7a) may be further simplified to

$$\ln Q = \frac{\beta\Delta}{2}\sum_{n=0}^{n_0}(Z_n+1)(2X_n-Z_n)\ , \tag{2.7b}$$

where Z_n is the integer part of X_n. Equation (2.7b) is especially convenient for the case where $Z_n \neq X_n$ for all n, i.e., no sublevel is exactly at the Fermi energy. Then, in differentiating $\ln Q$ with respect to various physical parameters, one has to account only for the derivatives of X_n in (2.7b) (no contributions from derivatives of n_0 or Z_n are to be accounted for). For example, in that case the number of particles N is given by

$$N = k_B T\frac{\partial \ln Q}{\partial \mu} = \sum_{n=0}^{n_0}(Z_n+1)\ , \tag{2.8}$$

and the magnetization M by

$$M = k_B T\frac{\partial \ln Q}{\partial H} = \frac{2\mu_B}{\hbar\omega_1}\sum_{n=0}^{n_0}(Z_n+1)[\tfrac{1}{2}\Delta(Z_n+1)-(n+\tfrac{1}{2})\hbar\omega]\ , \tag{2.9}$$

where $\mu_B \equiv e\hbar/2mc$. Note that the last result can be obtained by summing $-\partial E_{nm}/\partial H$ over all occupied levels. Equations (2.8) and (2.9) are correct only when $X_n \neq Z_n$. As the magnetic field (or some other external parameter) is varied, a sublevel may cross the Fermi energy. Such a crossing is accompanied by discontinuities in thermodynamic quantities. Using Eq. (2.7a), we find that the value of $\ln Q$ (and similarly of N and M) for an integer X_n $(=j)$, lies half-way between the values for $X_n \to j^+$ and $X_n \to j^-$. We will return to these discontinuities below. Figure 2 portrays the magnetization per particle as a function of $\hbar\omega_c$ (in arbitrary units, since M depends only on the ratios μ/Δ and $\hbar\omega/\Delta$) for a small number of occupied Landau levels and $\omega_c/\omega_0 \sim 4$–16. The division of M by N in Fig. 2 scales out the discontinuities in both M and N, leaving out a rich oscillating structure. The large-scale oscillations are those corresponding to the de Haas–van Alphen effect. These occur whenever n_0 changes (by unity) as the magnetic field is changed, and are clearly evident in Fig. 2. However, the confining potential leads to further, faster, oscillations, superimposed on the dHvA ones. In the following we concentrate upon the structure within a single dHvA oscillation, i.e., we assume that n_0 is constant. To this end we rewrite the second (oscillating) term in Eq. (2.7a) as

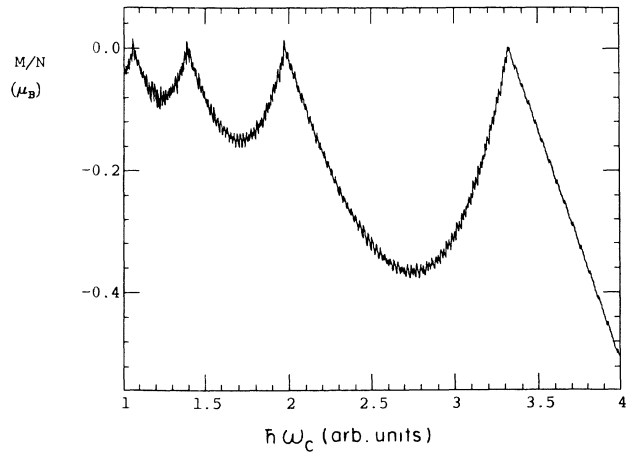

FIG. 2. The magnetization (in units of μ_B) in model I as a function of $\hbar\omega_c$ (in arbitrary units) for $\mu=5$ and $\omega_0=0.25$.

$$(\ln Q)_{\rm osc} = \sum_{p=1}^{\infty}\frac{\beta\Delta}{2\pi^2 p^2}\frac{\cos\{(2\pi p/\Delta)[\mu-\frac{1}{2}\Delta-\frac{1}{2}(n_0+1)\hbar\omega]\}\sin[(n_0+1)\pi p\hbar\omega/\Delta]}{\sin(\pi p\hbar\omega/\Delta)}\ . \tag{2.10}$$

Two types of oscillations (in addition to the dHvA oscillations!) are evident in (2.10). The first is related to the variation of μ/Δ by 1. Using Eq. (2.2) and $\Delta \sim (\hbar\omega_0)^2/\hbar\omega_c$, we find $\mu/\Delta \sim \phi/\phi_0$, where ϕ is the flux through the system of effective radius R, $\phi=\pi HR^2$. In other words, a variation of μ/Δ by unity corresponds to a variation of the flux by one flux quantum. These oscillations are of the Aharonov-Bohm type. Each period corresponds to one state per Landau level crossing the Fermi energy.[6] For a system of size $\sim 10^{-4}$ cm, the periodicity of the AB oscillations is of the order of 10 G. The discontinuity in the magnetization as a sublevel crosses the Fermi energy is determined by the magnetization of the states near this energy. It can be seen that it is largest for states belonging to the lowest $(n=0)$ and the highest $(n=n_0)$ Landau levels, and is of the order of $2\mu_B\mu/\hbar\omega \sim 2\mu_B n_0$. Thus, we expect these jumps to be larger for smaller magnetic fields, as is indicated in Fig. 2. Another behavior was obtained by Sivan and Imry,[6] who studied, in the WKB approximation, a *different* confining potential, namely a finite two-dimensional system bounded by infinite-potential walls. They obtained the magnetization of an edge state given by R/l_H, with $l_H=\sqrt{\hbar/m\omega_c}$, i.e., a magnetization that increases with increasing magnetic field. Our results, concurring with those obtained by Sivan and Imry, indicate that the magnitude of the AB oscillations depends on details of the confining potential.

The second kind of oscillations appearing in Eq. (2.10) is related to the variation of the factor $\hbar\omega/\Delta$ by 1. For strong magnetic fields, these oscillations are much slower (by a factor n_0) than the AB ones. The appearance of these oscillations can be attributed to the *correlations between different Landau levels,* in contrast with the AB oscillations which involve each Landau level separately. The energy difference between the bottom of the ladders belonging to adjacent Landau levels is $\hbar\omega$. Thus, as $\hbar\omega/\Delta$ increases by one, an additional sublevel in the

lower Landau level crosses (downward) the bottom of the higher Landau levels; otherwise, the two ladders retain the same interladder energy spacing. This means that the energy difference between a state, say, in the lower Landau level and the one closest in energy in a higher one, assumes nearly the same value as $\hbar\omega/\Delta$ is increased by unity, leading to the second kind of oscillations referred to above. In the general case, the amplitude of these oscillations should be of order $\sqrt{n_0}$. The correlation between Landau levels in this model may lead to a coherent AB effect, i.e., to a situation where sublevels in all Landau levels cross the Fermi energy simultaneously. This happens whenever $\hbar\omega/\Delta$ assumes an integer value; in that case, all (upper) sublevels of a given Landau level coincide with those of the lower ladders. This effect is manifested in Eq. (2.10), where an integer value of $\hbar\omega/\Delta$ leads to a factor of n_0+1. The oscillations of the second type are evidently a manifestation of the particular spectrum at hand. In more general models we expect these oscillations to be replaced by a "noisy" signal.

The spectrum has another interesting effect resulting from the correlation between different Landau levels. One may consider the distribution of level spacings $\{\delta\}$ between successive sublevels [belonging, according to the spectrum (2.4), to different Landau levels]. Were different Landau levels uncorrelated (e.g., each level was still described by a uniformly spaced ladder, but the shifts among different ladders were uncorrelated), this distribution would be Poisson-like, peaked at $\delta=0$. This, however, is not the case here. The distribution of $\{\delta\}$ for the spectrum (2.4), which may be regarded as that of two one-dimensional harmonic oscillators with incommensurate frequencies, has been studied in Ref. 10. It is sharply peaked around a finite value of δ. For example, studying this distribution for states near the Fermi energy, for the characteristic values depicted in Fig. 2 ($\mu=5$, $\hbar\omega_c=1$, and $\hbar\omega_0=0.1$, all in arbitrary units), we obtain the statistics of 1255 such energy gaps. The values $\delta\simeq 0.963\times 10^{-4}$ and $\delta\simeq 0.954\times 10^{-4}$ occur 656 and 144 times, respectively, which account for $\sim 64\%$ of the total distribution. Thus, if an absorption experiment could have been carried out on such a system, a sharp peak would be observed at this value of δ. It should be noted that the location of the peak of the distribution is very sensitive to the magnetic field. In Fig. 3 we display its dependence on $\hbar\omega_c$, for $\omega_0=0.25$, where only values of δ that account for more than 50% of the distribution are depicted. For very small changes of the magnetic field, the energy separation between nearest sublevels varies linearly with the field. One expects it to oscillate, with a period corresponding to the rate at which sublevels from adjacent Landau levels cross each other. A simple calculation shows that this period (in $\hbar\omega_c$) is equal to $\Delta/2$; this result is evident in Fig. 3, where $\Delta\simeq 0.06$. Due to the dependence upon the magnetic field, this quasigap is not manifested as oscillations in the thermodynamic functions. This is to be contrasted with the AB effect, which results from the constant gap Δ between adjacent sublevels in the same Landau level. In the latter, the gap remains practically constant over many periods of the AB oscillations.

So far we have discussed only thermodynamic quantities. We now turn to study a transport quantity, related to the quantized Hall effect. The current carried by a sublevel, characterized by n and l [see, e.g., Eq. (2.4a)], is given by[11]

$$I_{nl}=\frac{e}{h}\frac{\partial E_{nl}}{\partial l}\ . \tag{2.11}$$

Differentiating (2.4a), we find that the edge current (i.e., the current with the $\omega_0=0$ contribution subtracted) is equal to $\pm e\Delta/h$, where the plus (minus) sign corresponds to positive (negative) l. Since the energy separation Δ between states with positive l is much smaller than $\hbar\omega$, the energy separation between states with negative l, we expect that the states in an energy range ΔE will mainly carry a positive current. If ΔE is smaller than $\hbar\omega$, we can ignore the negative-l states and the overall current is

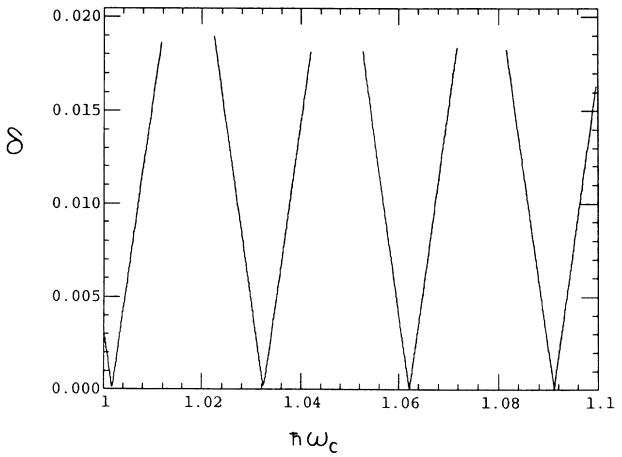

FIG. 3. The most frequent gap δ (see text) as a function of $\hbar\omega_c$ (both in arbitrary units). Only values of δ which account for more than half of the distribution are displayed.

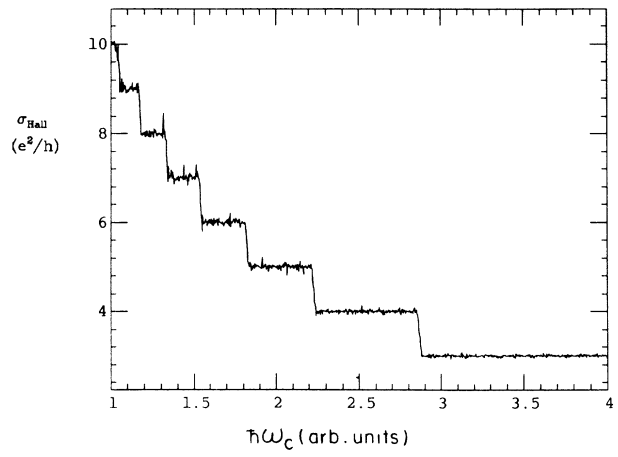

FIG. 4. Quantization of the Hall conductance (displayed here as a function of $\hbar\omega_c$). Aharonov-Bohm oscillations are superimposed on the Hall plateaus.

given by

$$I=(n_0+1)\frac{\Delta E}{\Delta}\frac{e\Delta}{h}=(n_0+1)\frac{e}{h}\Delta E\ , \tag{2.12}$$

where the factor $\Delta E/\Delta$ is the number of sublevels in each Landau level in the energy range ΔE. The guiding centers of the additional sublevels are located near $r=R$. Therefore, occupying $\Delta E/\Delta$ extra sublevels (per Landau level) may be viewed as raising the local Fermi level near the edge ($r=R$) by ΔE, i.e., applying transverse voltage of $\Delta E/e$. Hence, Eq. (2.12) leads to the usual quantization of the Hall conductance

$$\sigma_{\rm Hall}=(n_0+1)e^2/h\ .$$

This quantized Hall effect in the pure sample is the starting point of the discussion of the effect in disordered system.[4,11] It should be noted, however, that in obtaining (2.11) we have assumed a smooth density of states. Since the Hall current I is proportional to the number of states in the energy range ΔE, Eq. (2.11) suggests that AB oscillations occur on top of the Hall steps. Indeed, in Fig. 4, which displays the Hall current as a function of the magnetic field, AB oscillations are clearly observable.

III. EFFECTS OF SPIN-ORBIT INTERACTIONS: FIRST MODEL

In this section we study the effects of the s.o. interaction due to boundaries upon thermodynamic quantities. The s.o. interaction is obtained from Dirac's equation as a first-order relativistic correction [$O(v^2/c^2)$] to the Schrödinger equation

$$V_{\rm s.o.}=\frac{\hbar}{4m^2c^2}\sigma\cdot\left[\nabla V\times\left[\mathbf{p}-\frac{e\mathbf{A}}{c}\right]\right]\ , \tag{3.1}$$

where $\frac{1}{2}\hbar\sigma$ is the electron spin operator. With the harmonic confining potential $V(r)=\frac{1}{2}m\omega_0^2r^2$, the Hamiltonian in the presence of the s.o. interaction takes the form

$$\mathcal{H}=\frac{1}{2m}\left[\mathbf{p}-\frac{e\mathbf{A}}{c}\right]^2+\frac{m}{2}\omega_0^2r^2 +\frac{\hbar}{4m^2c^2}\sigma_z m\omega_0^2 r\left[\mathbf{p}-\frac{e\mathbf{A}}{c}\right]_\theta\ . \tag{3.2}$$

Using the gauge $\mathbf{A}=\frac{1}{2}\mathbf{H}\times\mathbf{r}$ and substituting, for each σ_z direction,

$$\Psi(r,\theta;\sigma_z)=\phi(r;\sigma_z)e^{il\theta}\ ,$$

it follows that ϕ satisfies the one-dimensional Schrödinger equation (2.3), with

$$\omega_1^2(\sigma_z)=\omega_c^2+4\omega_0^2-\Gamma\sigma_z\omega_0\omega_c\ , \tag{3.3a}$$

$$\omega_2(\sigma_z)=\omega_c-\tfrac{1}{2}\Gamma\sigma_z\omega_0\ , \tag{3.3b}$$

where Γ, which characterizes the magnitude of the s.o. interaction, is defined by $\Gamma=\hbar\omega_0/mc^2$. The energy levels for each value of σ_z ($\sigma_z=\pm1$) are given by (2.4) with the modified values of ω_1 and ω_2. For the above values of the parameters, Γ is extremely small ($\sim10^{-10}$). However, as discussed in the Introduction, this is related to the fact that the present model is characterized by a single parameter. In Sec. V we present an alternative model, which leads to much larger values of the s.o. parameter. Thus, in the following we discuss the influence of the s.o. interaction for arbitrary values of the s.o. parameter (though still small compared to unity).

The grand partition function is given again by Eq. (2.7), with the appropriate redefinitions of ω and Δ, and where an additional sum over the spin directions is implied. To linear order, the s.o. interaction does not affect the amplitude of the various terms in $\ln Q$, and consequently, in all thermodynamic quantities. Two interesting effects of the s.o. interaction are worth mentioning. First, through the dependence of n_0 on σ_z, one may observe a splitting of the dHvA oscillations which are prominent mainly near the maxima of the magnetization (see Fig. 2). In Fig. 5 we display this splitting for the overestimated value of $\Gamma=20\%$. Second, the s.o. coupling may also affect the AB oscillations. Expanding in the s.o. correction to Δ in the denominator of the argument of the cosine in (2.7a) leads to a multiplicative factor, given by $\cos(2\pi p\Gamma\mu/\hbar\omega_0)$. Due to the factor $\mu/\hbar\omega_0$, this term may still lead to a significant correction, even for small values of the s.o. coupling. Interestingly, this term is independent of the magnetic field and multiplies the AB oscillating term in all thermodynamic quantities. Thus, in some sense it may be considered "universal." This result is very similar to the universal multiplicative reduction factors, obtained in Ref. 12, due to s.o. scattering in disordered systems.

IV. CONFINING POTENTIAL: SECOND EXAMPLE

To examine to what extent the results of the previous model are sensitive to the particular choice of the confining potential, we consider a second model confined in the y direction by the potential

$$V(x,y)=\tfrac{1}{2}m\omega_0^2y^2\ , \tag{4.1}$$

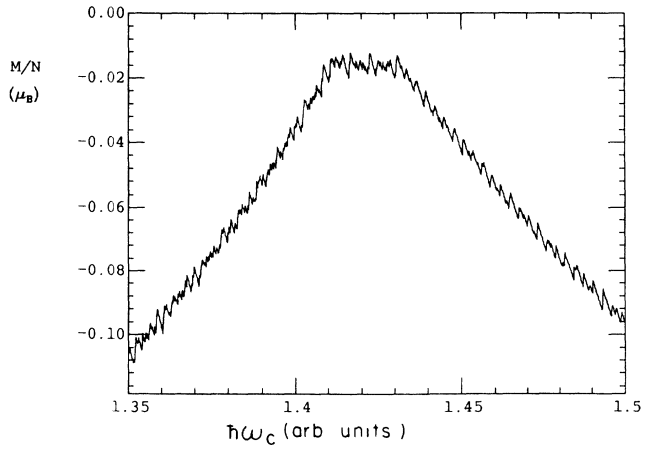

FIG. 5. The splitting of the magnetization peak (model I) in the presence of the s.o. interaction (compare with Fig. 2).

with periodic boundary conditions in the x direction,

$$\Psi(x+L_x,y)=\Psi(x,y) .$$

Again, ω_0, characterizing the confining potential, is chosen such that particles with potential energy near the Fermi energy μ experience an effective width L_y, $\mu\simeq\frac{1}{2}\omega_0^2 L_y^2$. As in Sec. II, $\omega_0\sim 10^{-10}$ 1/sec simulates reasonable ($L_y\sim 10^{-4}$ cm) systems. Self-consistent numerical studies[13] indicate that the potential (4.1) may faithfully describe the effective potential of quasi-one-dimensional (1D) systems with a magnetic field (mainly when a small number of Landau levels are occupied). This potential was also used by Xie and Das-Sarma[14] and by Kirczenow[15] to study transport in such quasi-1D systems.

We follow the procedure described in detail in the previous sections to obtain the spectrum, thermodynamic properties, and the current. Assuming the gauge $\mathbf{A}=-Hy\hat{x}$, we substitute for the wave function the form

$$\Psi(x,y)=\phi(y)e^{ik_x x} .$$

It then follows that $\phi(y)$ satisfies a one-dimensional Schrödinger equation with an effective harmonic potential

$$V_{\rm eff}=\frac{1}{2m}\frac{\omega_0^2(\hbar k_x)^2}{\omega^2}+\frac{m}{2}\omega^2(y-y_l)^2 , \tag{4.2}$$

with $\omega^2=\omega_c^2+\omega_0^2$ and $y_l=\omega_c\hbar k_x/m\omega^2$. Here $k_x=2\pi l/L_x$, l being an integer. The eigenenergies are given by

$$E_{nl}=(n+\tfrac{1}{2})\hbar\omega+\Delta l^2 , \tag{4.3}$$

where $\Delta=(h^2/2mL_x^2)\omega_0^2/\omega^2\equiv D_0\omega_0^2/\omega^2$. Using $H\sim 1$–10 T and $L_x\sim 10^{-4}$ cm, we have $\hbar\omega\sim 10^{-4}$–10^{-3} eV and $\Delta\sim 10^{-10}$–10^{-9} eV $\ll\hbar\omega$. The energy levels for $\omega_c/\omega_0=4$ are shown in Fig. 6.

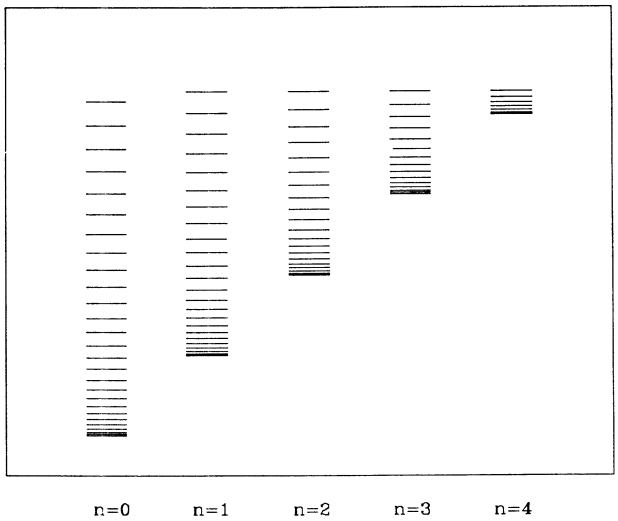

FIG. 6. Energy levels for model II for $\omega_c/\omega_0=4$ and $\omega_c/D_0=10$.

The grand partition function of this model is calculated exactly by employing the Poisson summation formula. We find (in the $T\to 0$ limit)

$$\ln Q=2\Delta\sum_{n=0}^{n_0}\left[\frac{2}{3}X_n^3+\sum_{p=1}^{\infty}\left[\frac{\sin(2\pi pX_n)}{2\pi^3p^3}-\frac{X_n\cos(2\pi pX_n)}{\pi^2p^2}\right]\right] , \tag{4.4}$$

with $X_n\equiv\{[\mu-(n+\frac{1}{2})\hbar\omega]/\Delta\}^{1/2}$ and n_0 is the maximal n such that $\mu-(n+\frac{1}{2})\hbar\omega$ is still positive. The magnetization M is obtained by differentiating with respect to the magnetic field

$$M=\sum_{n=0}^{n_0}\left\{-(n+\tfrac{1}{2})\hbar\omega'\left[2X_n+\sum_{p=1}^{\infty}\frac{2\sin(2\pi pX_n)}{\pi p}\right]+\Delta'\left[-\frac{2}{3}X_n^3+\sum_{p=1}^{\infty}\left[\frac{\sin(2\pi pX_n)}{\pi^3p^3}-\frac{2X_n\cos(2\pi X_n)}{\pi^2p^2}-\frac{2X_n^2\sin(2\pi pX_n)}{\pi p}\right]\right]\right\} , \tag{4.5a}$$

where the primes indicate derivatives with respect to the magnetic field

$$\omega'=\frac{2\mu_B}{\hbar\omega}\omega_c , \tag{4.5b}$$

$$\Delta'=-\frac{2\mu_B}{\hbar\omega}2\Delta\frac{\omega_c}{\omega} . \tag{4.5c}$$

For noninteger X_n, (4.5a) can be recast in the simpler form

$$M=\sum_{n=0}^{n_0}(2Z_n+1)\left[-(n+\tfrac{1}{2})\hbar\omega'-\frac{Z_n(Z_n+1)}{3}\Delta'\right]\equiv\sum_{n=0}^{n_0}M_n , \tag{4.6}$$

where Z_n is the integral part of X_n. In this case, the number of electrons in each Landau (n) level is $2Z_n+1$. Again, Eq. (4.6) may be obtained alternatively by summing the magnetizations of each level $-\partial E_{nl}/\partial H$ over all occupied levels states since, for a noninteger X_n, the number of occupied levels does not change with the field (i.e., it is considered as constant when differentiating with respect to the field). For an integer X_n, i.e., when a sublevel in the nth Landau level crosses the Fermi energy, the contribution of this level to the magnetization can be read from (4.5a) to be

$$M_n=-(n+\tfrac{1}{2})\hbar\omega'2Z_n-\frac{\Delta'}{3}(2Z_n^2+1)Z_n , \tag{4.7}$$

exactly midway between the values of M_n in (4.6) for

$(2Z_n-1)$ and for $(2Z_n+1)$ electrons in the nth Landau level, respectively.

For each Landau level, states with $l\sim 0$ lie in the center of the sample, while those with the maximal value of l, $l\sim Z_n$, lie near the boundary (defined by the Fermi energy). The magnetization of a bulk state (i.e., $l\sim 0$) is of the order of $2\mu_B(n+\frac{1}{2})$, while that of an edge state is

$$\sim 2\mu_B[2(n+\tfrac{1}{2})\hbar\omega-\mu]/\hbar\omega \ .$$

The latter is the order of magnitude of the jumps in the magnetization as a state crosses the Fermi level [cf. Eq. (4.7)]. It is seen that the contribution of the edge states is larger for the lowest and highest Landau levels. For those levels the magnetization due to boundary states is $\mu/\hbar\omega\sim n_0$ times larger than that of a bulk ($l\sim 0$) state. This result is similar to the one obtained for the magnetization of the edge states in the previous model. The magnetization per particle, for typical values of the parameters, is shown in Fig. 7. Comparing to Fig. 2, it is seen that the finite width of the sample in the x direction leads to an asymmetry between the decrease and increase of the magnetization. This is to be expected since, in the extreme case, namely, rigid boundary conditions in both directions, M is monotonically decreasing (with discontinuous jumps) as H is increasing, similar to the standard dHvA oscillations.

The AB oscillations are also evident in Fig. 7. Their period, from Eq. (4.5a), corresponds to a change of $X_n\sim(\mu/\Delta)^{1/2}$ by unity. Using $\mu\sim\frac{1}{2}mL_y^2\omega_0^2$ and the definition of Δ following Eq. (4.3), we again find the period ϕ/ϕ_0, where $\phi=HL_xL_y$. In this model, the sublevels in different Landau levels do not cross the Fermi energy coherently. Thus, in this case, the overall amplitude of the "noise" added to the dHvA oscillations [see discussion of the second kind of oscillations following Eq. (2.10)] will be of the order of $\sqrt{n_0}$ times that of the contribution of a single level.

Taking into account s.o. interaction due to the boundaries, one adds to the potential (4.1) the term

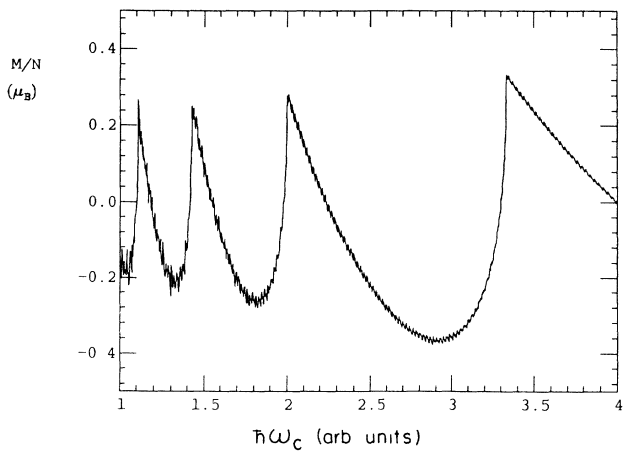

FIG. 7. The magnetization in model II as a function of $\hbar\omega_c$ (in arbitrary units) for $\mu=5$, $\omega_0=0.1$, and $D_0=0.1$.

$$V_{\text{s.o.}}=\frac{\hbar}{4m^2c^2}\sigma_z m\omega_0^2\, y\left[\hbar k_x+\frac{e}{c}Hy\right] . \tag{4.8}$$

The Hamiltonian can still be analytically diagonalized, leading, for each value of σ_z, to the same type of eigenenergies as in (4.3), but with modified frequency ω,

$$\omega^2=\omega_c^2+\omega_0^2+\sigma_z\frac{\hbar\omega_0}{2mc^2}\omega_0\omega_c \ .$$

Δ is unaltered to first order in the s.o. coupling strength. We see that the modifications due to the s.o. interaction are of the same order and of the same kind as those discussed in detail in Sec. III and consequently lead to similar effects.

As mentioned above, the present model, defined by Eq. (4.1), may be used to investigate transport properties in quasi-1D systems.[14,15] To this end we calculate the current $I_x^{(nl)}$, carried by the state Ψ_{nl} along the x direction,

$$I_x^{(nl)}=\frac{e}{mL_x}\left\langle\Psi_{nl}\left|\hbar k_x+\frac{eHy}{c}\right|\Psi_{nl}\right\rangle . \tag{4.9a}$$

A straightforward calculation leads to

$$I_x^{(nl)}=\frac{eh}{mL_x^2}\frac{\omega_0^2}{\omega^2}l \ . \tag{4.9b}$$

We see that in the presence of a magnetic field, it is the confinement in the y direction that accounts for a current in the x direction. This, indeed, will vanish when $\omega_0=0$. (Without a magnetic field the current is independent of ω_0). One may imagine[15] that the states with positive k_x (and l) carry currents which originate from a reservoir in the far negative-x region, while those with negative k_x originate from a corresponding reservoir in the positive-x direction. If one assigns different chemical potentials to these two reservoirs, μ_1 and μ_2, then a net current will flow in the system

$$I_x=\sum_{n=0}^{n_0}\sum_{l=l_1}^{l_2}I_x^{(nl)}\simeq(n_0+1)\frac{e}{h}(\mu_2-\mu_1) \ , \tag{4.10}$$

where l_i is the integral part of

$$X_i\equiv\{[\mu_i-(n+\tfrac{1}{2})\hbar\omega]/\Delta\}^{1/2} \ ;$$

the right-hand side (rhs) of Eq. (4.10) is obtained when the difference between l_i and X_i is neglected. The chemical potential difference and the current are both in the x direction. Equation (4.10)—in the particular case of zero magnetic field—is a manifestation of the quantization of the conductance in constricted ballistic systems.[8,9] Such a quantization holds, in this model, even when a magnetic field is turned on. It is interesting to note that the role of independent channels is played here by the harmonic levels, i.e., the quantum number n, which, in the presence of a magnetic field, denotes the Landau levels. In other words, the number of independent channels is the number of occupied harmonic levels. This interplay between magnetic and electric depopulation of subbands was

indeed observed.[16] We note that the quantization (4.10) persists even in the absence of a magnetic field (where now the number of channels will be given by the number of the harmonic-oscillator states below the Fermi energy). This is in contrast with Ref. 15, but in accordance with the interpretation presented in Ref. 17. When the difference between l_i and X_i is taken into account, AB oscillations appear on top of the quantization (4.10), similarly to the AB oscillations exhibited in Fig. 4.

In order to study the Hall effect in this system, it is convenient to write (4.9) as

$$I_x^{(nl)}=-\frac{e}{m\omega_c L_x}\frac{1}{1+\omega_0^2/\omega_c^2}\frac{\partial E_{nl}}{\partial y_l} . \tag{4.11}$$

It is interesting to note that if one defines $-\partial E_{nl}/\partial y_l$ as an "effective" electric force acting on the electron at state Ψ_{nl}, then Eq. (4.11), apart from a small finite-size correction, yields a "classical" Hall effect for this state. If one applies a chemical potential difference in the y direction, then the current in the x direction is given by[4,11]

$$I_x=\sum_{n=0}^{n_0}\sum_{y_l} I_x^{(nl)}=\frac{n_0+1}{\Delta(y_l)}\int dy_l I_x^{(nl)}$$

$$=(n_0+1)\frac{e}{h}\Delta\mu , \tag{4.12}$$

where $\Delta(y_l)=y_l-y_{l-1}$ and we have used (4.11) to obtain the last equality in (4.12). We note from (4.11) that a potential difference in the y direction induces a current in the x direction only in the presence of a magnetic field, in agreement with the interpretation of (4.12) as the quantized Hall effect (in ordered systems). This effect can be measured provided that the coupling between opposite edge states, which carry currents of opposite directions, is neglected. Again we expect AB oscillations to be superimposed on these steps.

V. SPIN-ORBIT INTERACTION IN WKB APPROXIMATION

In the previous sections we have presented an exact calculation of the grand partition function for two confining potentials in the presence of the s.o. interaction due to the boundaries. For parameters appropriate for mesoscopic samples we concluded that the modifications due to this interaction were rather small. While being exactly solvable, these confining potentials are governed by a single parameter, ω_0, that determines both the width of the sample and the potential gradient near the boundary (i.e., at $E\sim\mu$). This is in contrast with real systems, where these two characteristics are expected to be independent. One may expect that, since the s.o. interaction is proportional to the potential gradient, increasing the gradient, while keeping the system size unchanged, may lead to a stronger s.o. interaction. This cannot be achieved in the context of the models discussed so far. We thus introduce another model defined by the confining potential

$$V(y)=\begin{cases}0, & 0\le y\le L_y ,\\ \alpha(y-L_y), & L_y\le y ,\end{cases} \tag{5.1}$$

with $V(y)=V(-y)$ and periodic boundary conditions $[\Psi(x,y)=\Psi(x+L_x,y)]$ in the x direction. We carry out a WKB calculation of the energy levels of this two-dimensional model. Choosing the gauge $\mathbf{A}=(-Hy,0,0)$ and substituting

$$\Psi(x,y;\sigma_z)=\phi(y;\sigma_z)e^{ik_x x}$$

with $k_x=2\pi l/L_x$, one obtains a one-dimensional Schrödinger equation for $\phi(y;\sigma_z)$, with the effective potential

$$V_{\rm eff}(y)=\tfrac{1}{2}m\omega_c^2(y-y_l)^2+V(y)$$
$$+\Theta(|y|-L_y)C_{\rm s.o.}(\sigma_z)\hbar k_x\alpha , \tag{5.2}$$

where $y_l=-\hbar k_x/m\omega_c$ and $C_{\rm s.o.}=\sigma_z\hbar/4m^2c^2$, arising from the s.o. interaction due to the boundaries in the y direction. Here $\Theta(y)$ is the Heavyside function. In obtaining (5.2) we have neglected $e\mathbf{A}/c$ compared to $\mathbf{p}$ in the s.o. interaction term, which is justified in the range of magnetic fields considered in this paper. The Bohr-Sommerfeld quantization condition for the energy levels is given by

$$(n+\tfrac{1}{2})\pi=\frac{1}{\hbar}\int_{c_1}^{c_2}\sqrt{2m[E-V_{\rm eff}(y)]}\,dy , \tag{5.3}$$

where c_1 and c_2 are the classical turning points, i.e., the values of y where the integrand vanishes. For a bulk state [i.e., $|y_l|<L_y-\sqrt{2E/\hbar\omega_c}\,l_H$, with $l_H\equiv\sqrt{\hbar/(m\omega_c)}$], $V_{\rm eff}(y)=\frac{1}{2}m\omega_c^2(y-y_l)^2$ in the entire range of integration. Then c_1 and c_2 are given by

$$c_{1,2}=y_l\mp\sqrt{(2E/\hbar\omega_c)}\,l_H , \tag{5.4}$$

and (5.3) yields $E_{nl}=(n+\frac{1}{2})\hbar\omega_c$, the infinite system solutions. For an edge state, either c_1 or c_2 are determined by the boundary of the system. For example, for an edge state near the right-hand side of the system, the quantization condition (5.2) becomes

$$(n+\tfrac{1}{2})\pi=\frac{1}{\hbar}\int_{c_1}^{L_y}\{2m[E-\tfrac{1}{2}m\omega_c^2(y-y_l)^2]\}^{1/2}dy+\frac{1}{\hbar}\int_{L_y}^{c_2}\{2m[E-\tfrac{1}{2}m\omega_c^2(y-y_l)^2-\alpha(y-a)-C_{\rm s.o.}\hbar k_x\alpha]\}^{1/2}dy , \tag{5.5}$$

where c_1 is given by (5.4) and c_2 is the value of y where the second integrand vanishes. Carrying out the integrals in (5.5), we obtain a transcendental equation for the energy levels. The first integral gives

$$I_1=\frac{E}{\hbar\omega_c}[\cos^{-1}(z_l)-z_l(1-z_l^2)^{1/2}] , \tag{5.6}$$

with $z_l=\sqrt{\hbar\omega_c/2E}\,(y_l-L_y)/l_H$. In the case of infinite

walls at $y=\pm L_y$, I_1 would be the complete answer[5,6,17,18] (note that, in that case, $c_2=L_y$).

Assuming steep boundaries ($\alpha l_H \gg \hbar\omega_c$), we now discuss the $z_l \ll 1$ case. [The case $(1-z_l)\ll 1$ is not realistic here for when $(y_l-L_y)/l_H \gg 1$, the effective potential is dominated by $\alpha(y_l-L_y)$, which, in turn, leads to $z_l \ll 1$.] We expand the two integrals in (5.5) to first order in z_l, $\hbar\omega_c/\alpha l_H$, and $C_{\text{s.o.}}\hbar k_x \alpha/E$, to find

$$E_{nl}=2(n+\tfrac{1}{2})\hbar\omega_c\left[1+\frac{2}{\pi}\left[3z_l-\sqrt{4(n+\tfrac{1}{2})}\frac{\hbar\omega_c}{\alpha l_H}+\frac{3}{2\sqrt{n+\frac{1}{2}}}\frac{C_{\text{s.o.}}\hbar k_x}{l_H}\right]\right]. \tag{5.7}$$

(A similar result, without the s.o. interaction, was obtained in Ref. 5.) Some consequences of Eq. (5.7) concerning the s.o. interaction are worth mentioning. The relative energy shift due to the s.o. interaction does not depend on α in this approximation. This is related to the fact that, as the potential gradient increases, the range over which it affects the wave function decreases at the same rate, leading to an energy shift independent of the potential gradient. We also note that, using the definition of $C_{\text{s.o.}}$ following Eq. (5.2) and noting that, for the edge states under consideration $\hbar k_x \simeq m\omega_c L_y$, the magnitude of the s.o. splitting takes the form $[(\hbar\omega_c/mc^2)(L_y/l_H)]$. Comparing to the estimates of the s.o. splitting obtained in the previous sections, we find the following: (a) The s.o. splitting is proportional to $\hbar\omega_c/mc^2$ (compared to $\hbar\omega_0/mc^2$ in the previous models), which is at least 1 or 2 orders of magnitude larger. (b) The factor L_y/l_H leads to further enhancement of the s.o. term (for example, for $H\sim 10$ T and $L_y\sim 10^{-4}$ cm, $L_y/l_H\sim 100$). (c) The splitting increases as $H^{3/2}$ due to the appearance of l_H in the denominator. Thus, although the effect is rather small for the present set of parameters (of the order of 10^{-6}–10^{-5}), it may still be measured when higher magnetic fields and larger (ballistic) systems become available.

VI. DISCUSSION

We have examined two types of confining potentials which may simulate small, finite-size, mesoscopic systems. In both cases, the confining potential lifts the degeneracy of the Landau levels and consequently leads to an oscillatory behavior as a function of the magnetic field superimposed upon the dHvA oscillations. This is manifested in the magnetization per particle (Figs. 2 and 7) and should be observed in other thermodynamic properties as well.

Turning to transport quantities, we have found that the Landau levels play the role of the "independent channels" in the Landauer picture.[19] This was obtained for the longitudinal as well as for the transverse conductivity. Moreover, AB oscillations appear on top of the quantized conductance steps (see, e.g., Fig.4).

Both confining potentials yield qualitatively similar results, though the statistical properties of the energy spectra are quite different. Some features of these models may be shared by clean, mesoscopic samples. The effect of static disorder, including magnetic impurities, is left for a future study.

We have concluded that the detailed form of the confining potential appears to be rather irrelevant, as far as thermodynamic and transport properties are concerned. These depend upon a restricted number of energy levels around the Fermi energy, and hence are rather insensitive to the global details of the energy spectrum. The results may therefore be relevant to experiments in such ballistic constricted geometries.

Particular attention was paid to the effect of s.o. interaction due to the boundaries. It is found that, due to the s.o. coupling, the oscillating terms in the thermodynamic quantities are multiplied by a factor which depends upon the parameters of the system and is independent of the magnetic field. This result is amenable to experimental verification. Admittedly, the s.o. coupling is rather small for the examples considered. However, its effect on various thermodynamic quantities that exhibit oscillations with the magnetic field is "universal,"[12] and hence may be detected in experiments. Also, one expects splitting, due to the s.o. coupling, in the dHvA oscillations, which may also be detected in experiments. Zeeman splitting is represented by an additional term in the Hamiltonian. Since it does not connect spin-up and spin-down electrons, it only gives rise to trivial degeneracy lifting of the spectrum. This conclusion has to be revised, of course, when static scattering potential is introduced.

ACKNOWLEDGMENTS

This work was supported in part by the U.S.-Israel Binational Science Foundation, the Minerva Foundation (Munich), the Fund for Basic Research administered by the Israel Academy of Sciences and Humanities, and by the German-Israeli Foundation.

[1]N. W. Ashcroft and N. D. Mermin, *Solid State Physics* (Saunders College, Philadelphia, 1976).

[2]K. v. Klitzing, G. Dorda, and M. Pepper, Phys. Rev. Lett. **45**, 494 (1980).

[3]Ch. Sikorskii and U. Merkt, Phys. Rev. Lett. **62**, 2164 (1989); W. Hansen, J. P. Smith, III, K. Y. Lee, J. A. Brun, C. M. Knoedler, J. M. Hong, and D. I. Kern, *ibid.* **62**, 2168 (1989).

[4]A. MacDonald and P. Streda, Phys. Rev. B **29**, 1616 (1984).

[5]É. N. Bogachek and G. A. Gogadze, Zh. Eksp. Teor. Fiz. **63**, 1839 (1972) [Sov. Phys.—JETP **36**, 973 (1973)].

[6]U. Sivan and Y. Imry, Phys. Rev. Lett. **61**, 1001 (1988).

[7]Y. Aharonov and D. Bohm, Phys. Rev. **115**, 485 (1959).

[8]B. J. van Wees, H. van Houten, C. W. J. Beenakker, J. G. Williamsen, L. P. Kouwenhoven, D. van der Marel, and C. T.

Foxon, Phys. Rev. Lett. **60**, 848 (1988); D. A. Wharam, T. J. Thornton, R. Newbury, M. Pepper, H. Ahmed, J. E. F. Frost, D. G. Hasko, D. C. Peacock, D. A. Ritchie, and G. A. C. Jones, J. Phys. C **21**, L209 (1988).

[9]Y. Imry, in *Directions in Condensed Matter Physics,* edited by G. Grinstein and G. Mazenko (World-Scientific, Singapore, 1986).

[10]M. V. Berry and M. Tabor, Proc. R. Soc. London Ser. A **356**, 375 (1977).

[11]B. I. Halperin, Phys. Rev. B **25**, 2185 (1982).

[12]Y. Meir, Y. Gefen, and O. Entin-Wohlman, Phys. Rev. Lett. **63**, 798 (1989).

[13]S. E. Laux and F. Stern, Appl. Phys. Lett. **49**, 91 (1986); P. F. Maldague, Bull. Am. Phys. Soc. **26**, 787 (1981); S. E. Laux, D. J. Frank, and F. Stern, Surf. Sci. **196**, 101 (1988).

[14]X. Xie and S. Das-Sarma, Solid State Commun. **26**, 787 (1987).

[15]G. Kirczenow, Phys. Rev. B **38**, 10 958 (1988).

[16]B. J. van Wees, L. P. Kouwenhoven, H. van Houten, C. W. J. Beenakker, J. E. Mooij, C. T. Foxon, and J. J. Harris, Phys. Rev. B **38**, 3625 (1988).

[17]R. B. Dingle, Proc. R. Soc. London **216A**, 118 (1953); **219A**, 463 (1953).

[18]T. W. Nee and R. E. Prange, Phys. Lett. **25A**, 582 (1967); R. E. Prange and T. W. Nee, Phys. Rev. **168B**, 779 (1968).

[19]R. Landauer, IBM J. Res. Dev. **1**, 223 (1957).